Inorganic Chemistry

ARTICLE

pubs.acs.org/IC

# On the Structural and Electronic Properties of $[Zn_2(4,4'\text{-bipyridine})(mes)_4]^{n-}$ ($n = 0-2$), a Homologous Series of Bimetallic Complexes Bridged by Neutral, Anionic, and Dianionic 4,4′-Bipyridine

Mark Irwin, Tobias Krämer, John E. McGrady, and Jose M. Goicoechea*

Department of Chemistry, Inorganic Chemistry Laboratory, University of Oxford, South Parks Road, Oxford OX1 3QR, U.K.

Supporting Information

**ABSTRACT:** Addition of 1 equiv of potassium metal to a tetrahydrofuran (THF) solution of $Zn_2(4,4'\text{-bipyridine})(mes)_4$ (**1**; mes =2,4,6-$Me_3C_6H_2$) in the presence of 18-crown-6 (1,4,7,10,13,16-hexaoxacyclooctadecane) yielded the radical anionic species $[Zn_2(4,4'\text{-bipyridine})(mes)_4]^{\bullet-}$, which was characterized by single crystal X-ray diffraction in $[K(18\text{-crown-6})(THF)_2][Zn_2(4,4'\text{-bipyridine})(mes)_4]$ (**2**). A similar reaction employing 2 equiv of alkali metal afforded the related complex $[K(18\text{-crown-6})]_2[Zn_2(4,4'\text{-bipyridine})(mes)_4]$ (**3**). The $[Zn_2(4,4'\text{-bipyridine})(mes)_4]^{n-}$ ($n = 0-2$) moieties present in **1**−**3** are largely isostructural, yet exhibit significant structural variations which arise because of differences in their electronic structure. These species represent a homologous series of complexes in which the ligand exists in three distinct oxidation states. Structural data, spectroscopic measurements, and density functional theory (DFT) calculations are consistent with the assignment of **1**, **2**, and **3** as complexes of the neutral, radical anionic, and dianionic 4,4′-bipyridyl ligand, respectively. To the best of our knowledge, species **2** and **3** are the first crystallographically characterized transition metal complexes of the 4,4′-bipyridyl radical and dianion.

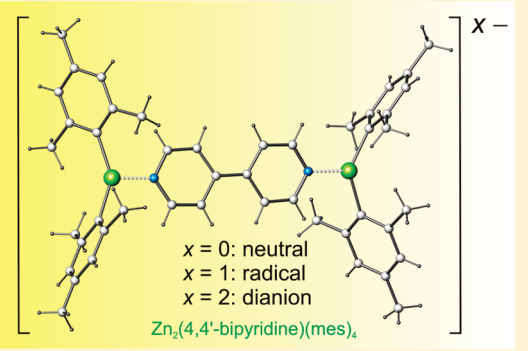


## INTRODUCTION

The redox-active behavior of 4,4′-bipyridine has been well established for over 50 years. Early electron paramagnetic resonance (EPR) studies on organic radicals in solution were the first to identify the 4,4′-bipyridyl anion ($4,4'\text{-bipy}^{\bullet-}$) as a product of the reduction of pyridine, or 4,4′-bipyridine, with alkali metals.[1,2] Further studies on the radical anion and dianion were later conducted by several research groups employing a combination of spectroscopic, electrochemical, and computational techniques.[3−5] Electrochemical measurements on solutions of 4,4′-bipyridine reveal two consecutive chemically accessible reduction steps, highlighting the possibility of forming coordination complexes of these highly reductive species.[3,4] The use of 4,4′-bipyridine in molecular squares exhibiting ligand-centered mixed valency (LCMV) has been reported by Hupp and others, who have demonstrated that the electrochemical reduction of neutral supramolecular complexes can give rise to isostructural species where negative charges reside on bridging ligand moieties.[6] However, despite the extensive research in this area, to the best of our knowledge there are no structural data available in the chemical literature for coordination complexes with chemically reduced forms of the 4,4′-bipyridyl ligand. Our research group recently reported the isolation and crystallographic characterization of the 4,4′-bipyridyl radical anion and dianion as alkali metal salts,[7] and herein we report a follow-up study on the covalently bonded Lewis acid−base adducts of these species.

Our interest in such complexes stems from reports that transition metal complexes of open-shell "non-innocent" ligand systems may exhibit unique reactivity when compared to closely related complexes with ligand systems which are not redox-active.[8] Numerous examples of non-innocent ligands have been reported in the literature and include semiquinone and phenoxyl systems,[9,10] dithiolates,[11] α-diimines,[12] α-iminopyridines,[13] α-iminoketones,[14] tetrazenes,[15] aminyl radicals,[16] and imino- and thio-phenolates.[17] Similar "non-innocent" behavior has also been established for the 2,2′-isomer of bipyridine.[8b−d]

Herein we report the isolation and electronic characterization of $[Zn_2(4,4'\text{-bipyridine})(mes)_4]$ (**1**) as well as of the $[K(18\text{-crown-6})]^+$ salts of the anionic, $[K(18\text{-crown-6})(THF)_2][Zn_2(4,4'\text{-bipyridine})(mes)_4]$ (**2**), and dianionic, $[K(18\text{-crown-6})]_2[Zn_2(4,4'\text{-bipyridine})(mes)_4]$ (**3**), derivatives and apply single-crystal X-ray diffraction, electron paramagnetic resonance (EPR), and NMR spectroscopy and density functional theory (DFT) to characterize their electronic structures. These physiochemical measurements are consistent with the presence of a 4,4′-bipyridyl radical anion in **2**, and of the 4,4′-bipyridyl dianion in **3**.

## EXPERIMENTAL SECTION

**General Methods.** All reactions and product manipulations were carried out under an inert atmosphere employing standard Schlenk-line

**Received:** February 4, 2011
**Published:** May 03, 2011



  

or glovebox techniques. Toluene (99.9%, Rathburn Chemicals, Ltd.) and hexanes (99.9%, Rathburn Chemicals, Ltd.) were dried using an MBraun SPS-800 solvent purification system. Tetrahydrofuran (THF; 99.9%, Rathburn Chemicals, Ltd.) was distilled over potassium metal under a dinitrogen atmosphere. All solvents were stored in gastight ampules under argon. In addition, toluene and hexanes were stored over activated 3 Å molecular sieves (Acros). Potassium metal (99.95%, Aldrich) was stored under dinitrogen in an MBraun UNIlab glovebox maintained at <0.1 ppm $H_2O$ and <0.1 ppm $O_2$ and used as received. 4,4′-Bipyridine (>99%, Acros) and 18-crown-6 (1,4,7,10,13,16-hexaoxacyclooctadecane; 99%, Alfa-Aesar) were used as delivered after being carefully dried under vacuum. $Zn(mes)_2$ (mes = 2,4,6-$Me_3C_6H_2$) was synthesized according to a modified literature-reported procedure (see Supporting Information for details).[18]

*$Zn_2$(4,4′-bipyridine)(mes)$_4$* (**1**). $Zn(mes)_2$ (300 mg, 0.988 mmol) and 4,4′-bipyridine (77 mg, 0.494 mmol) were dissolved in THF (~4 mL) under an inert atmosphere and stirred for 5 h, forming a pale yellow solution. The resulting solution was filtered and layered with hexanes. Large colorless needle-like crystals of $Zn_2$(4,4′-bipyridine)$(mes)_4$ formed overnight in good yields (240 mg, 63.6% crystalline yield). A powder X-ray diffraction pattern was obtained which matched the simulated diffraction pattern based on the single-crystal X-ray diffraction data (Supporting Information, Figure S1). Anal. Calcd. for $C_{46}H_{52}N_2Zn_2$: C 72.34%, H 6.86%, N 3.67%. Found: C 72.25%, H 6.77%, N 3.58%. $^1$H NMR (299.9 MHz, $d_8$-THF): $\delta$ (ppm) 8.57 (d, 4H, *ortho*-4,4′-bipyridyl, $^3J_{H-H}$ = 6 Hz), 7.71 (d, 4H, *meta*-4,4′-bipyridyl, $^3J_{H-H}$ = 6 Hz), 6.73 (s, 8H, $C_6H_2(CH_3)_3$), 2.42 (s, 24H, *ortho*-$CH_3$), 2.21 (s, 12H, *para*-$CH_3$). The $^1$H NMR spectrum of **1** was assigned with the help of a COSY 2-D experiment. $^{13}$C NMR (75.4 MHz, $d_8$-THF): $\delta$ (ppm) 152.59 (s, *ipso*-$C_6H_2(CH_3)_3$), 151.45 (s, *ortho*-4,4′-bipyridyl), 147.05 (s, *para*-4,4′-bipyridyl), 145.48 (s, *ortho*-$C_6H_2(CH_3)_3$), 136.52 (s, *para*-$C_6H_2(CH_3)_3$), 126.48 (s, *meta*-$C_6H_2(CH_3)_3$), 122.88 (s, *meta*-4,4′-bipyridyl), 27.42 (s, *ortho*-$CH_3$), 21.58 (s, *para*-$CH_3$). $^{13}C\{^1H\}$ NMR resonances were assigned with the help of HSQC and HMBC 2-D spectra. See Figures S2−S7 of the Supporting Information for NMR spectra. IR (cm$^{-1}$): 515 (w), 540 (m), 580 (w), 629 (s), 668 (w), 710 (w), 721 (w), 809 (s), 818 (s), 845 (s), 965 (w), 971 (w), 984 (w), 1005 (s), 1042 (m), 1070 (m), 1099 (w), 1215 (s), 1262 (w), 1285 (w), 1317 (w), 1412 (m), 1506 (w), 1525 (w), 1531 (w), 1539 (w), 1558 (w), 1570 (w), 1578 (w), 1602 (s). Raman (cm$^{-1}$): 1637 (w), 1613 (m), 1605 (w), 1513 (w), 1381 (w), 1350 (w), 1298 (w), 1290 (m), 1290 (m), 1233 (w), 1176 (w), 1019 (m), 1015 (m), 944 (w), 770 (w), 658 (w), 580 (m), 552 (m), 397 (w), 332 (w), 298 (w). IR and Raman data are provided in Supporting Information, Figures S8 and S9.

*[K(18-crown-6)(THF)$_2$][$Zn_2$(4,4′-bipyridine)(mes)$_4$]* (**2**). A mixture of **1** (100 mg, 0.131 mmol), potassium metal (5 mg, 0.130 mmol), and 18-crown-6 (35 mg, 0.131 mmol) was dissolved in THF (5 mL) under an inert atmosphere giving rise to a deep blue solution. The reaction mixture was stirred overnight, filtered, and layered with hexanes. The mixture was allowed to slowly diffuse at a temperature between 8 and 10 °C over the course of several days, ultimately affording dark blue block-like crystals of [K(18-crown-6)(THF)$_2$][$Zn_2$(4,4′-bipyridine)$(mes)_4$] in good yields (115 mg, 72% crystalline yield). The crystals obtained from the THF/hexane solvent mixture proved to be suitable for single crystal X-ray diffraction and were found to contain two crystalline phases of identical composition (**2a** and **2b**). A powder X-ray diffraction pattern collected on the solid isolated from this reaction was found to only contain **2a** and **2b** (Supporting Information, Figure S10). The X-band (9.3896 GHz) CW room-temperature EPR spectrum of a solid sample of **2** revealed a strong resonance with a *g* value of 2.0039. Anal. Calcd. for $C_{66}H_{92}KN_2O_8Zn_2$: C 65.42%, H 7.66%, N 2.31%. Found: C 61.60%, H 6.94%, N 2.73%. CHN elemental analyses results consistently showed low concentrations of carbon and hydrogen. IR (cm$^{-1}$): 539 (w), 578 (w), 618 (m), 668 (w), 687 (w), 772 (m), 775 (m), 780 (w), 834 (w), 841 (m), 963 (s), 1020, (s), 1038 (w), 1103 (s), 1131 (w), 1171 (w), 1198 (s), 1220 (w), 1235 (w), 1248 (w), 1283 (m), 1350 (m) 1547 (w), 1592 (s). Raman (cm$^{-1}$): 1630 (s), 1514 (s), 1352 (s), 1236 (s), 1047 (s), 1015 (m), 751 (m), 712 (w), 688 (w), 427 (w), 387 (w). IR and Raman data are provided in Supporting Information, Figures S8 and S9.

*[K(18-crown-6)]$_2$[$Zn_2$(4,4′-bipyridine)(mes)$_4$]* (**3**). In a typical reaction, a mixture of **1** (100 mg, 0.131 mmol), potassium metal (10 mg, 0.263 mmol), and 18-crown-6 (69.8 mg, 0.264 mmol) was dissolved in anhydrous THF (5 mL) under an inert atmosphere. The reaction mixture initially takes on a deep blue color which, when stirred overnight, gives rise to a dark yellow/brown solution. The reaction mixture was filtered and layered with hexanes. After several days dark brown plate-like crystals of [K(18-crown-6)]$_2$[$Zn_2$(4,4′-bipyridine)$(mes)_4$] were obtained in high yields (141 mg, 81.9% crystalline yield). Anal. Calcd. for $C_{70}H_{100}K_2N_2O_{12}Zn_2$: C 61.34%, H 7.35%, N 2.04%. Found: C 61.28%, H 7.20%, N 1.87%. $^1$H NMR (299.9 MHz, $d_8$-THF): $\delta$ (ppm) 6.50 (s, 8H, $C_6H_2(CH_3)_3$), 5.92 (d, 4H, *ortho*-4,4′-bipyridyl, $^3J_{H-H}$ = 6 Hz), 4.51 (d, 4H, *meta*-4,4′-bipyridyl, $^3J_{H-H}$ = 6 Hz), 3.57 (s, 48H, 18-crown-6), 2.32 (s, 24H, *ortho*-$CH_3$), 2.21 (s, 12H, *para*-$CH_3$). The $^1$H NMR spectrum of **3** also exhibits some resonances arising from a $[Zn(mes)_3]^-$ impurity at 6.40 (s, 6H), 2.28 (s, 18H, *ortho*-$CH_3$), 2.08 (s, 9H, *para*-$CH_3$). $^{13}$C NMR (125.8 MHz, $d_8$-THF) $\delta$/ppm: 161.48 (s, *para*-$C_6H_2(CH_3)_3$), 145.20 (s, *ortho*-$C_6H_2(CH_3)_3$), 139.78 (s, *ortho*-4,4′-bipyridyl), 132.88 (s, *ipso*-$C_6H_2(CH_3)_3$), 124.92 (s, *meta*-$C_6H_2(CH_3)_3$), 105.45 (*para*-4,4′-bipyridyl), 104.42 (s, *meta*-4,4′-bipyridyl), 72.01 (broad, s, 18-crown-6), 27.56 (s, *ortho*-$CH_3$), 21.56 (s, *para*-$CH_3$). The $^{13}$C NMR spectrum of **3** also exhibits some resonances arising from a $[Zn(mes)_3]^-$ impurity at 170.05 (s, *para*-$C_6H_2(CH_3)_3$), 145.31 (s, *ortho*-$C_6H_2(CH_3)_3$), 131.14 (s, *ipso*-$C_6H_2(CH_3)_3$), 124.55 (s, *meta*-$C_6H_2(CH_3)_3$), 72.01 (broad, s, 18-crown-6), 26.73 (s, *ortho*-$CH_3$), 21.75 (s, *para*-$CH_3$). $^{13}C\{^1H\}$ NMR resonances were tentatively assigned with the help of HSQC and HMBC 2-D spectra. See Figures S11−S16 of the Supporting Information for NMR spectra. IR (cm$^{-1}$): 668 (w), 722 (m), 801 (s), 841 (m), 934 (w), 949 (w), 962 (w), 983 (m), 1031 (w), 1109 (s), 1170 (w), 1197 (m), 1216 (w), 1252 (w), 1260 (w), 1284 (w), 1351 (m), 1506 (w), 1539 (w), 1559 (w), 1577 (w), 1608 (w). Raman (cm$^{-1}$): 1612 (s), 1507 (s), 1349 (s), 1233 (w), 1077 (w), 1046 (s), 1007 (w), 989 (w), 742 (w). IR and Raman data are provided in Supporting Information, Figures S8 and S9.

*[K(18-crown-6)(THF)][Zn(mes)$_3$]* (**4**). THF (~5 mL) was added to a sample vial containing $Zn(mes)_2$ (100.1 mg, 0.329 mmol), potassium metal (~13.0 mg, ~0.332 mmol), and 18-crown-6 (90.4 mg, 0.342 mmol) in a glovebox. This initially formed a colorless solution, which became pale brown after about 5 min. This was stirred overnight before filtering off a dark precipitate (assumed to be elemental Zn), and the remaining light brown solution was layered with hexanes. After several days colorless block-like crystals of [K(18-crown-6)(THF)][Zn$(mes)_3$] formed, suitable for single crystal X-ray diffraction (111.1 mg, 42.3% crystalline yield). A powder X-ray diffraction pattern was obtained which matched the simulated diffraction pattern for **4** based on the single-crystal X-ray diffraction data (Supporting Information, Figure S17). Anal. Calcd. for $C_{39}H_{57}KO_6Zn$ (**4**-THF): C 64.47%, H 7.91%. Found: C 64.08%, H 7.67%. (Note: There is a THF molecule present in the crystal structure which is believed to be lost on sealing the solid sample under vacuum). $^1$H NMR (299.86 MHz, $d_8$-THF): $\delta$ (ppm) 6.41 (s, 6H, $C_6H_2(CH_3)_3$), 3.57 (s, 24H, 18-crown-6), 2.28 (s, 18H, *ortho*-$CH_3$), 2.09 (s, 9H, *para*-$CH_3$). $^{13}$C NMR (125.80 MHz, $d_8$-THF) $\delta$/ppm: 170.05 (s, *para*-$C_6H_2(CH_3)_3$), 145.31 (s, *ortho*-$C_6H_2(CH_3)_3$), 131.14 (s, *ipso*-$C_6H_2(CH_3)_3$), 124.55 (s, *meta*-$C_6H_2(CH_3)_3$), 72.01 (broad, s, 18-crown-6), 26.73 (s, *ortho*-$CH_3$), 21.75 (s, *para*-$CH_3$). See Figures S18 and S19 of the Supporting Information for NMR spectra.

**X-ray Diffraction.** Single-crystal X-ray diffraction data were collected using an Enraf-Nonius Kappa-CCD diffractometer and a 95 mm

CCD area detector with a graphite-monochromated molybdenum $K_\alpha$ source ($\lambda$ = 0.71073 Å). Crystals were selected under Paratone-N oil, mounted on MiTeGen loops and quench-cooled using an open flow $N_2$ cooling device.[19] Data were processed using the DENZO-SMN package, including unit cell parameter refinement and interframe scaling (which was carried out using SCALEPACK within DENZO-SMN).[20] Structures were subsequently solved using direct methods, and refined on $F^2$ using the SHELXL 97-2 package.[21]

Transmission powder X-ray patterns were recorded using a Siemens D5000 diffractometer in modified Debye−Scherrer geometry equipped with an MBraun position sensitive detector. The instrument produced Cu $K_{\alpha1}$ radiation ($\lambda$ = 1.54056 Å) using a germanium monochromator and a standard Cu source. Data were recorded on samples in flame-sealed capillaries under dinitrogen. The capillaries were mounted on a goniometer head and aligned so that rotation occurred along the long central axis of the capillary. During a measurement the capillary was rotated at ∼60 rpm to minimize any preferred orientation effects that might occur.

**NMR.** $^1$H and $^{13}$C NMR spectra were acquired at 299.9 and 75.4 MHz, respectively, on a Varian Mercury-vx 300 NMR spectrometer. The $^{13}$C NMR spectrum of **3** was recorded at 125.8 MHz on a Bruker AVII 500 spectrometer equipped with a $^{13}$C cryoprobe. $^{13}$C and $^1$H spectra were referenced to $d_8$-THF ($\delta$ 25.37 ppm) and to the most shielded residual protic solvent resonance (THF $\delta$ 1.73 ppm), respectively. Diffusion and NOE experiments were performed on a Bruker AVII 500 spectrometer equipped with a TXI inverse probe regulated at 298 K. Diffusion experiments utilized the BPP-LED stimulated echo sequence with diffusion times ($\Delta$) of 50 ms, bipolar diffusion-encoding field gradient pulses of total duration 4 ms ($\delta$) and longitudinal eddy current delays (LED) of 5 ms.[22] Additional 0.6 ms purging gradients were applied whenever magnetization was longitudinal. All gradient pulses were of half-sine profiles with effective diffusion-encoding gradient strengths ranging from 0.5 to 20.5 G cm$^{-1}$ (corrected for half-sine profiles). Data analysis was performed using Bruker TOPSPIN software. 1D NOESY spectra were recorded using a single pulsed field gradient selective excitation scheme utilizing a 40 ms selective Gaussian inversion pulse and with a NOE mixing time of 0.8 s.

**Computational Methods.** All calculations presented in this paper were carried out with the Gaussian 09 program package at the DFT level of theory.[23] Geometries of the complexes **1**−**3** were fully optimized without imposing any symmetry constraints ($C_1$ symmetry), employing the M05−2X hybrid meta exchange-correlation functional developed by Truhlar and co-workers.[24] The M05−2X functional has been recommended for use with Zn compounds and in the present study afforded slightly better geometries compared to B3LYP. All stationary points were confirmed to be genuine minima by analytical calculation of their harmonic vibrational frequencies. Ahlrichs' TZVP basis set was used on Zn and all coordinating atoms (N and C1 of mesityl groups), while the SVP basis set was used on the remaining atoms.[25] The topological properties of electronic densities, obtained at the same level of theory, were characterized using the Atoms In Molecules (AIM) theory of Bader with the AIM2000 program package.[26,27]

$^1$H chemical shifts were calculated with the Gauge-Independent Atomic Orbital (GIAO) method,[28] using the geometries calculated at the M05−2X/TZVP/SVP level, as described above. These calculations were done with the B3LYP functional,[29] with a basis set optimized for shielding constants, aug-pcS-2 (triple-$\zeta$ quality) on the hydrogen atoms of the bipyridine moiety and one mesityl group,[30] which was used as internal standard. For the remaining atoms the same basis sets as defined above were used (TZVP on Zn and coordinating atoms, SVP for all other atoms). Relative chemical shifts ($\delta$) were obtained by referencing the nuclear magnetic shielding constants of the probe atoms against the arithmetic mean of the isotropic magnetic shielding constants of the *ortho*-methyl protons. These appear as an intense singlet in the experimental NMR spectrum with a chemical shift of 2.42 and 2.32 ppm for complexes **1** and **3**, respectively. Nucleus-Independent Chemical Shifts (NICS) values were calculated at the same level using the GIAO method as recommended by Schleyer et al.[31] The NICS probes (ghost atoms) were placed 1 Å above the centers of the rings (defined as the average of the Cartesian coordinates of the ring atoms). The NICS(1) values largely reflect the influence of $\pi$-electrons, and are therefore a better indicator of the ring current (aromaticity) than the values at the center, where $\sigma$-bonding contributions are also of importance.

**Additional Characterization Techniques.** IR data were recorded on solid samples in Nujol mulls. The mulls were made up inside an inert atmosphere glovebox and the KBr plates placed in an airtight container prior to data collection. Spectra were recorded on a Nicolet Magna-IR 560 spectrometer in absorbance mode (Happ-Genzel FT apodization) with a Ge/CsI beam splitter and liquid nitrogen cooled Mercury Cadmium Telluride (MCT) detector.

Raman spectra were recorded on solid samples under dinitrogen in flame-sealed Pyrex capillaries using a Dilor Labram 300 spectrometer. The excitation radiation was produced by a 20 mW helium−neon laser operating at a wavelength of 632.817 nm. Optical density filters could be inserted into the beam to reduce photon flux, decreasing the likelihood that photochemical reactions would take place during the measurement. Typically measurements were obtained at 1% of full intensity with a counting time of 120 s. Calibration of the spectrometer was performed before each measurement by referencing to the 520.7 nm line of a silicon wafer.

CW EPR experiments were performed using an X-band Bruker BioSpin GmbH EMX spectrometer equipped with a high sensitivity Bruker probe head. Experiments were conducted with 2−10 mW microwave power, 0.1 mT modulation amplitude, and a modulation frequency of 100 kHz. The magnetic field was calibrated at room temperature with an external 2,2-diphenyl-1-picrylhydrazyl standard ($g$ = 2.0036). Solid state spectra were recorded on approximately 2 mg of sample in flame-sealed quartz capillaries. Solution phase spectra were recorded on 0.1 mM solutions in dry THF.

CHN elemental analyses were performed on 5 mg samples submitted under vacuum in flame-sealed Pyrex ampules.

## RESULTS AND DISCUSSION

**Synthesis.** The complex $Zn_2$(4,4′-bipyridine)(mes)$_4$ (**1**) was synthesized by direct reaction of 4,4′-bipyridine (4,4′-bipy) with Zn(mes)$_2$ (mes = 2,4,6-$Me_3C_6H_2$) in a 1:2 ratio in anhydrous tetrahydrofuran (THF). A compositionally pure white crystalline solid can be isolated in high yields (>60%) by layering a THF solution of **1** with hexanes. The purity of **1** was confirmed by multielement NMR spectroscopy, powder X-ray diffraction (see Supporting Information), and elemental analysis. No other products were observed for this reaction. Single-crystal X-ray diffraction measurements reveal two dimesitylzinc moieties that are bridged by a 4,4′-bipy ligand (Figure 1a). Crystallographic data and experimental parameters for the structure are presented in Table 1. There are numerous Zn/4,4′-bipyridine complexes in the field of coordination polymer/metal−organic framework chemistry;[32] however, discrete two-to-one species in which two zinc nuclei are bridged by a single 4,4′-bipyridine ligand are much rarer.[33] Rarer still are 4,4′-bipyridine-bridged homoleptic organometallic zinc complexes, none of which have been structurally characterized to date.[34]

Reduction of **1** with 1 equiv of potassium metal in THF in the presence of 18-crown-6 (1,4,7,10,13,16-hexaoxacyclooctadecane) was found to yield a dark blue solution from which [K(18-crown-6)(THF)$_2$][$Zn_2$(4,4′-bipy)(mes)$_4$] (**2**) was isolated. The compositional

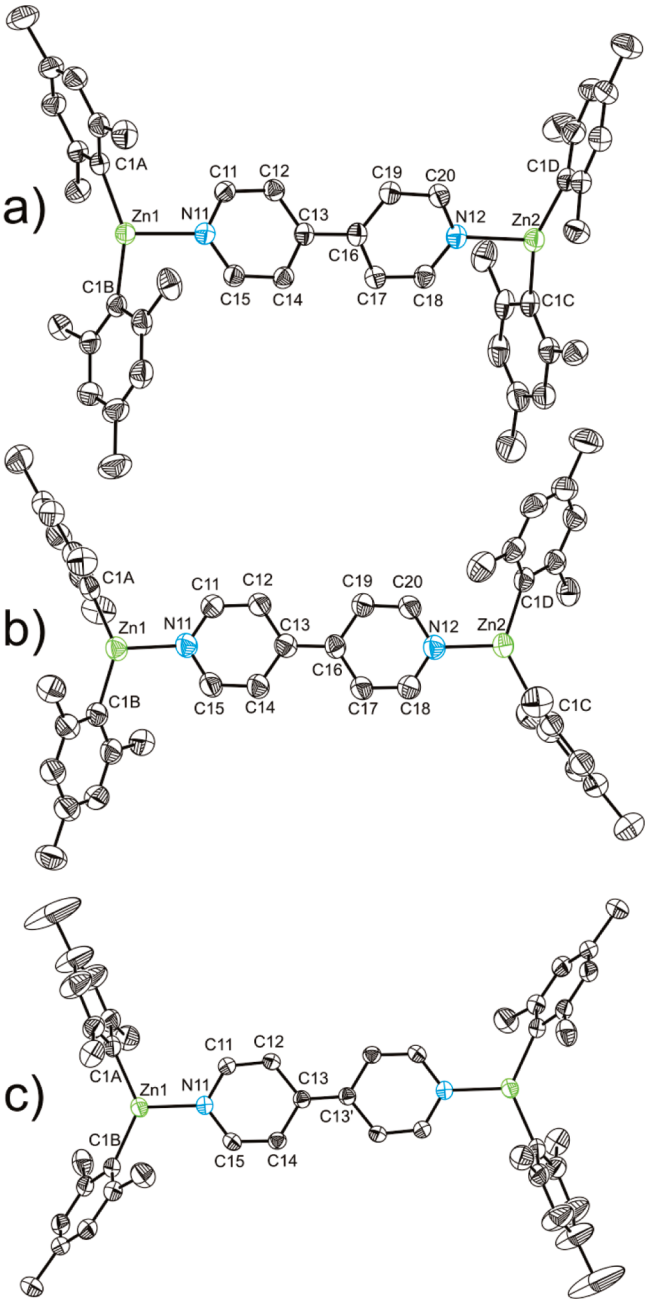


**Figure 1.** Thermal ellipsoid plots of (a) one of the two crystallographically unique $Zn_2(4,4'\text{-bipy})(mes)_4$ units present in the asymmetric unit of **1**; (b) one of the $[Zn_2(4,4'\text{-bipy})(mes)_4]^{\bullet-}$ radical anions present in **2a**; (c) the $[Zn_2(4,4'\text{-bipy})(mes)_4]^{2-}$ dianion present in **3** (a crystallographic center of inversion sits between C13 and C13′). All hydrogen atoms have been omitted for clarity. Anisotropic displacement ellipsoids are pictured at the 50% probability level.

purity of a solid sample of **2** was confirmed by powder X-ray diffraction. The results obtained from elemental analyses show lower carbon and hydrogen content than would be expected, perhaps because of a noncrystalline contaminant or the poor combustion of sample **2**. **2** can be obtained as a mixture of two polymorphic crystalline samples (**2a** and **2b**) by layering a THF solution of **2** with hexanes. Both species contain an anionic moiety, $[Zn_2(4,4'\text{-bipy})(mes)_4]^{\bullet-}$, which is the result of a single electron reduction of the neutral parent compound. The radical anion is accompanied in the lattice by a $[K(18\text{-crown-}6)(THF)_2]^+$ countercation. The anion exhibits a very similar structure to that of complex **1** (see Figure 1b). Bimetallic complexes in which metal centers are bridged by a 4,4′-bipyridyl radical anion have been previously proposed in the chemical literature;[35] however, to our knowledge, **2** represents the first example of such a species for which X-ray structural data is available.

A similar reaction as used for the synthesis of **2**, but using 2 equiv of potassium metal, was found to yield a dark brown solution from which $[K(18\text{-crown-}6)]_2[Zn_2(4,4'\text{-bipy})(mes)_4]$ (**3**) was isolated. The crystal structure of **3** reveals a dianionic $[Zn_2(4,4'\text{-bipy})(mes)_4]^{2-}$ species (Figure 1c) which is accompanied in the lattice by two $[K(18\text{-crown-}6)]^+$ cations. Species **3** was shown to be compositionally pure in the solid-state by elemental analysis and powder X-ray diffraction. Solution NMR spectra of this sample also show that the dianion is relatively stable to decomposition although trace amounts of a minor impurity, consistent with the presence of the $[Zn(mes)_3]^-$ anion, were observed in the $^1H$ and $^{13}C$ NMR spectra. The dianion exhibits a very similar structure to that of the $Zn_2(4,4'\text{-bipy})(mes)_4$ moieties present in **1** and **2**. A comparison of bond metric parameters for all three samples **1**−**3** is provided in Table 2.

During the course of these studies it was also observed that the direct reduction of $Zn(mes)_2$ with potassium metal in the absence of 4,4′-bipyridine yielded the previously reported anionic species, $[Zn(mes)_3]^-$ (Figure 2), in high yields.[36] The trimesitylzinc(II) anion was isolated from solution as a salt of $[K(18\text{-crown-}6)(THF)]^+$, in $[K(18\text{-crown-}6)(THF)][Zn(mes)_3]$ (**4**).

**Bond Metric Data.** Complexes **1**−**3** all contain $[Zn_2(4,4'\text{-bipy})(mes)_4]^{n-}$ ($n = 0, 1, 2$) units in which two dimesitylzinc(II) centers are bridged by a 4,4′-bipyridyl moiety. The most pronounced structural changes to these three species are observed for the interatomic Zn−N distances which are 2.183(av), 2.043(av), and 1.977(2) Å for compounds **1**, **2**, and **3**, respectively. This is consistent with an increased degree of electrostatic character to the Zn−N bond and has the effect of moderately weakening the bonds between the Zn(II) centers and the strongly $\sigma$-donating mesityl substituents (manifested in a lengthening of the Zn−C bonds). A similar effect, albeit less pronounced, has been reported by our research group for the Fe/2,2′-bipyridine systems $[Fe(2,2'\text{-bipy})(mes)_2]^{n-}$ ($n = 0, 1$).[37] The second most pronounced structural change, and the most meaningful, is to the bond distances between pyridyl rings of the 4,4′-bipy moieties. These distances are significantly shortened on going from the neutral complex (1.482(av) Å) to the radical (1.420(av) Å) and dianionic (1.373(4) Å) analogues. The degree of contraction of this C−C bond is very similar to that observed in recent studies on the reduction of the 2,2′- and 4,4′-isomers of bipyridine to the corresponding anions and dianions.[7,38] The lowest unoccupied molecular orbital (LUMO) of 4,4′-bipyridine, which becomes occupied upon reduction, is a $\pi^*$ antibonding orbital with an in-phase relationship between the p orbitals on the carbon atoms linking the two rings (as pictured in Figure 3b). This in-phase relationship implies a greater degree of double bond character in the reduced species. Because of the ubiquitous use of 4,4′-bipyridine in the field of metal organic framework chemistry it is also worth highlighting that reduction of the ligand has a cumulative effect on the Zn−Zn distances in these systems which shorten from 11.435(av) Å in **1**, to 11.232(av) Å for **2**, and finally to 11.187(1) Å in **3**.


dx.doi.org/10.1021/ic200241d |*Inorg. Chem.* 2011, 50, 5006–5014

**Table 1. Selected X-ray Data Collection and Refinement Parameters for $[Zn_2(4,4'\text{-bipyridine})(mes)_4]$ (1), $[K(18\text{-crown-6})(THF)_2][Zn_2(4,4'\text{-bipyridine})(mes)_4]$ (2a and 2b), $[K(18\text{-crown-6})]_2[Zn_2(4,4'\text{-bipyridine})(mes)_4]$ (3), and $[K(18\text{-crown-6})(THF)][Zn(mes)_3]$ (4)**

| compound | 1 | 2a | 2b | 3 | 4 |
|---|---|---|---|---|---|
| formula | $C_{46}H_{52}N_2Zn_2$ | $C_{66}H_{92}KN_2O_8Zn_2$ | $C_{66}H_{92}KN_2O_8Zn_2$ | $C_{70}H_{100}K_2N_2O_{12}Zn_2$ | $C_{43}H_{65}KO_7Zn$ |
| Fw | 763.64 | 1211.26 | 1211.26 | 1370.46 | 798.42 |
| space group, $Z$ | $P\bar{1}$, 4 | $P\bar{1}$, 4 | $P\bar{1}$, 6 | $P2(1)/c$, 2 | $Pbcn$, 8 |
| $a$ (Å) | 11.3857(1) | 19.7748(3) | 20.6965(1) | 11.7304(2) | 33.6475(2) |
| $b$ (Å) | 19.2169(2) | 20.6378(3) | 20.8215(1) | 13.8528(2) | 10.7686(1) |
| $c$ (Å) | 19.5817(2) | 21.1360(3) | 27.0298(1) | 22.4989(4) | 24.2059(1) |
| α (deg) | 83.461(1) | 118.439(1) | 76.111(1) | 90.0 | 90.0 |
| $\beta$ (deg) | 80.452(1) | 109.127(1) | 81.897(1) | 92.474(1) | 90.0 |
| $\gamma$ (deg) | 73.809(1) | 98.547(1) | 61.729(1) | 90.0 | 90.0 |
| $V$ (Å$^3$) | 4047.15(7) | 6666.9(2) | 9953.6(1) | 3652.6(1) | 8770.7(1) |
| $\rho_{calc}$ (g cm$^{-3}$) | 1.253 | 1.207 | 1.212 | 1.246 | 1.209 |
| radiation, $\lambda$ (Å), temp (K) | | | Mo K$_\alpha$, 0.71073, 150(2) | | |
| $\mu$ (mm$^{-1}$) | 1.218 | 0.833 | 0.837 | 0.828 | 0.700 |
| reflections collected | 35531 | 41137 | 89021 | 15136 | 19056 |
| independent reflections | 18473 | 23111 | 45306 | 8264 | 9975 |
| R(int) | 0.0286 | 0.0403 | 0.0261 | 0.0329 | 0.0250 |
| R1/wR2,[a] $I \geq 2\sigma_I$ (%) | 3.88/9.62 | 4.78/12.41 | 4.71/11.66 | 4.54/9.98 | 4.07/10.37 |
| R1/wR2,[a] all data (%) | 5.51/10.45 | 7.04/13.61 | 7.08/13.09 | 7.85/11.25 | 6.45/11.37 |

[a] $R1 = \Sigma||F_o| - |F_c||/\Sigma|F_o|$; $wR2 = \{\Sigma w(F_o^2 - F_c^2)^2/\Sigma w(F_o^2)^2\}^{1/2}$; $w = [\sigma^2(F_o)^2 + (AP)^2 + BP]^{-1}$, where $P = [(F_o)^2 + 2(F_c)^2]/3$ and the $A$ and $B$ values are 0.0505 and 1.62 for **1**, 0.0674 and 1.62 for **2a**, 0.0588 and 6.40 for **2b**, 0.0476 and 1.95 for **3**, and 0.0551 and 4.67 for **4**.

**Table 2. Mean Bond Distances [Å] and Angles [deg] for the $[Zn_2(4,4'\text{-bipy})(mes)_4]$ Moieties Crystallographically Characterized in 1−3 and the Optimized Computed Geometries**

| | | neutral | | radical | | | dianion | |
|---|---|---|---|---|---|---|---|---|
| bond[a] | 4,4′-bipy[b] | 1 | $\mathbf{1}_{DFT}$ | 2a | 2b | $\mathbf{2}_{DFT}$ | 3 | $\mathbf{3}_{DFT}$ |
| **1** | 1.335 | 1.342 | 1.33 | 1.361 | 1.359 | 1.36 | 1.379 | 1.38 |
| **2** | 1.377 | 1.383 | 1.39 | 1.363 | 1.366 | 1.37 | 1.354 | 1.36 |
| **3** | 1.386 | 1.394 | 1.40 | 1.426 | 1.425 | 1.43 | 1.465 | 1.47 |
| **4** | 1.484 | 1.482 | 1.48 | 1.417 | 1.423 | 1.43 | 1.373(4) | 1.38 |
| Zn−N | N/A | 2.183 | 2.24 | 2.043 | 2.043 | 2.07 | 1.977(2) | 1.97 |
| Zn-mes | N/A | 1.975 | 2.01 | 1.987 | 1.992 | 2.03 | 2.004 | 2.06 |
| torsion | 17.23 | 35.25 | 38.2 | 2.83 | 2.40 | 0.0 | 0.00 | 0.0 |
| N−Zn−C | N/A | 103.32 | 100.1 | 111.12 | 111.44 | 109.6 | 114.33 | 117.1 |
| C−Zn−C | N/A | 153.26 | 159.8 | 137.69 | 137.05 | 140.9 | 131.33(10) | 125.8 |

[a] Bond numbering scheme as indicated in Figure 3a. [b] Data taken from a survey of the 3197 crystallographically characterized species containing 4,4′-bipyridine for which metric data is reported in the Cambridge Structural Database at the time of preparation of this manuscript.

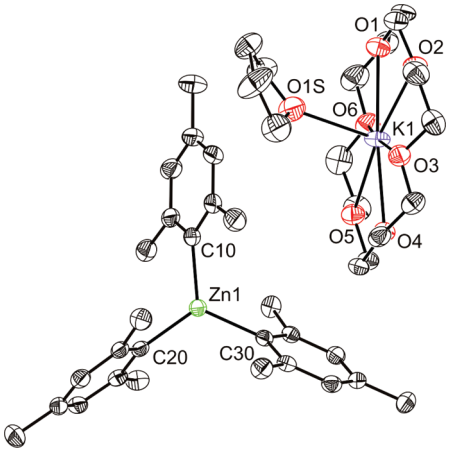


**Figure 2.** Thermal ellipsoid plot of the atoms present in the asymmetric unit of **4**. All hydrogen atoms and minor component arising from some crystallographic disorder of the THF molecule have been omitted for clarity. Anisotropic displacement ellipsoids are pictured at the 50% probability level.

We have optimized the geometries of complexes $\mathbf{1}_{DFT}$ ($S = 0$), $\mathbf{2}_{DFT}$ ($S = 1/2$), and $\mathbf{3}_{DFT}$ ($S = 0$) in the indicated electronic states. For complex $\mathbf{3}_{DFT}$ we have also located an excited triplet state, which has not been considered further, because of the high energy separation (+43 kcal mol$^{-1}$) from the ground state. In all cases, the optimized geometries obtained using DFT were found to be in line with the crystallographically determined data (see Table 2). The C−C and C−N bond distances are within ±0.01 Å of their experimental counterparts, while the Zn−N and Zn−C interactions are typically overestimated by 0.02−0.06 Å. Upon reduction of the neutral species to the anionic and dianionic forms, the Zn−N distances contract from 2.24 to 2.07 and 1.97 Å (for complexes $\mathbf{1}_{DFT}$, $\mathbf{2}_{DFT}$ and $\mathbf{3}_{DFT}$, respectively) compared to 2.18, 2.04, and 1.98 Å for **1**, **2** and **3**, respectively. At the same time the Zn−C interactions are weakened (2.01, 2.03, and 2.06 Å). The C−C bridge between the two pyridyl rings of the 4,4′-bipyridine ligand also contracts considerably upon reduction from 1.48 Å to 1.43 Å and 1.38 Å, as a result of successive occupation of the LUMO of the neutral ligand (Figure 3). Thus, the character of this central bond changes from a single to a double bond in the dianionic species. The same trend is apparent for bond 2 (according to the numbering scheme employed in Figure 3), although the contraction is less pronounced compared


dx.doi.org/10.1021/ic200241d |*Inorg. Chem.* 2011, 50, 5006–5014

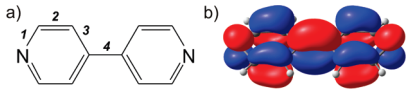


**Figure 3.** (a) Numbering scheme employed to discuss metric bond data for all of the 4,4′-bipyridine containing species. (b) The 4,4′-bipyridine LUMO which clearly shows antibonding interactions for bonds 1 and 3 and bonding interactions for bonds 2 and 4.

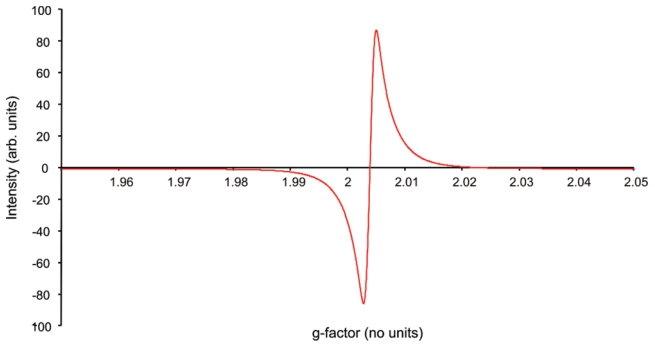


**Figure 4.** X-band (9.3896 GHz) CW EPR spectrum of a solid sample of **2** recorded at 296 K.

to the interpyridyl bond. Conversely, bonds 1 and 3 follow the opposite trend, lengthening upon reduction. The higher degree of $\pi$ overlap in the central bond also enforces coplanarity of the two pyridyl moieties, the optimum torsion angle being reduced from 38.2° in $\mathbf{1}_{\mathbf{DFT}}$ to 0.0° in both $\mathbf{2}_{\mathbf{DFT}}$ and $\mathbf{3}_{\mathbf{DFT}}$. A spin density plot for the radical anionic complex $\mathbf{2}_{\mathbf{DFT}}$ is provided in the Supporting Information, Figure S20.

## MAGNETIC RESONANCE STUDIES (NMR AND EPR)

EPR spectra were recorded for samples **2** and **3**. The EPR spectrum of a solid sample of **2** reveals a strong resonance at room temperature with a *g* value of 2.0039 (Figure 4). This resonance is relatively sharp as would be expected for an organic radical anion and is very similar to that observed for solid samples of the alkali metal salts of the 4,4′-bipyridyl radical anion such as Na(4,4′-bipy)(en) ($g$ = 2.0043 in the solid state).[7] The spectrum of a solid sample of **3** reveals a much weaker resonance at a similar *g* value which we attribute to trace amounts of the 4,4′-bipyridyl anion present in the sample. **3** is extremely air- and moisture-sensitive, and we believe that in recording the EPR spectrum some sample decomposes to give rise to the radical anion.

The solution phase EPR spectrum of a THF solution of **2** reveals a complex asymmetric resonance exhibiting extensive hyperfine coupling (Supporting Information, Figure S21). All of our attempts to model this resonance have thus far proven unsuccessful. We believe that the observed spectrum is a composite of two resonances arising from two distinct paramagnetic species. The most significant component of such a resonance is the $[Zn_2(4,4'\text{-bipy})(mes)_4]^{\bullet-}$ radical anion present in the crystal structure of **2**. Diffusion NMR data for the neutral analogue **1** (vide infra) indicate that the bipyridyl-bridged structure observed in the solid state is largely intact in solution; however, a minor amount of ligand dissociation is also likely to be present. At the high dilution limits required for solution phase EPR spectrometry the degree of dissociation of $[Zn_2(4,4'\text{-bipy})(mes)_4]$ to $Zn(mes)_2$ and 4,4′-bipyridine is expected to be more pronounced (an increased effective concentration of THF is likely to favor heavily solvated $Zn(mes)_2$). Such dissociation is also likely to be present for sample **2** and **3**. In the case of a THF solution of **2**, this would give rise to an additional contribution to the EPR spectrum arising from the free 4,4′-bipyridyl radical anion. The spectrum of the 4,4′-bipyridyl radical anion has previously been reported by us and others and found to have a *g* value of 2.00439.[1,2,7] The overlap of both such resonances gives rise to the asymmetric spectrum we have recorded. Because of the extensive hyperfine coupling which is expected for both contributing species, deconvolution and modeling of the observed spectrum has proved unviable. These results were reproducible and observed on each occasion a solution phase sample of **2** was studied.

$^1$H and $^{13}C\{^1H\}$ NMR spectroscopic studies of a $d_8$-THF solution of **1** indicate that the two-to-one structure which is observed in the solid-state remains intact in solution with little evidence of ligand dissociation. The $^1$H NMR spectrum of **1** reveals five resonances at 8.57, 7.71, 6.73, 2.42, and 2.21 ppm. The two resonances at 8.57 and 7.71 ppm correspond to the *ortho*- and *meta*- 4,4′-bipyridyl protons, respectively. These resonances are shifted with respect to free 4,4′-bipyridine (8.69 and 7.67 ppm). As would be expected, the resonances arising from the mesityl moieties occur at very similar chemical shifts to the $Zn(mes)_2$ precursor (6.71, 2.45, 2.20 ppm). To confirm that the structure of **1** remains intact in solution and that there is no significant ligand dissociation, a one-dimensional NOESY spectrum on a $d_8$-THF solution of **1** was conducted. The resonance arising because of the mesityl *ortho*-methyl groups (2.42 ppm) was selectively inverted which resulted in the enhancement of the signal intensities for the mesityl *meta*-protons and the 4,4′-bipyridyl *ortho*-protons, consistent with the bridged structure remaining intact in solution. The resonance arising from the 4,4′-bipyridyl *meta*-protons was enhanced to a much lesser degree than those in the *ortho*-positions indicating that they are more distant from the *ortho*-methyl groups of the mesityl functionalities. Additional room-temperature (298 K) diffusion experiments on $Zn(mes)_2$, 4,4′-bipyridine and **1** were also conducted to establish the structure of **1** in solution (Supporting Information, Figure S7). The diffusion coefficient values ($D$) determined for **1** show that those arising from 4,4′-bipyridyl resonances ($1.132 \times 10^{-9}$ and $1.133 \times 10^{-9}$ m$^2$/s for the *ortho*- and *meta*-protons, respectively) are very close in magnitude to those arising from the $Zn(mes)_2$ moieties ($1.027 \times 10^{-9}$, $1.021 \times 10^{-9}$, and $1.031 \times 10^{-9}$ m$^2$/s, for the *meta*-protons, the *ortho*-methyl, and *para*-methyl substituents, respectively). The small discrepancy in the values obtained for the diffusion coefficients indicates that if there is any dissociation of **1** to give 2 equiv of $Zn(mes)_2$ and 4,4′-bipyridine in solution, the equilibrium lies strongly shifted toward species **1**. This assumption is further supported by the observation that the observed $D$ values are significantly different to those obtained for a solution of 4,4′-bipyridine of the same molarity ($1.911$ and $1.913 \times 10^{-9}$ m$^2$/s for the *ortho*- and *meta*-protons, respectively).

The $^1$H NMR spectrum of sample **3** (which is contaminated by a small amount of **4**) reveals a significant shift of the 4,4′-bipyridyl resonances with respect to the values observed for the neutral parent compound **1** from 8.57 and 7.71 ppm to 5.92 and 4.51 ppm for **1** and **3**, respectively. A comparison of the $^1$H NMR spectra of **1** and **3** is provided in the Supporting Information, Figure S16. The chemical shift values observed for **3** are consistent with those previously reported for the only known


dx.doi.org/10.1021/ic200241d |*Inorg. Chem.* 2011, 50, 5006–5014

example of a complex of the 2,2′-bipyridyl dianion, [{Yb($\mu^2$-$N_2C_{10}H_8$)$(THF)_2$}$_3$], which were reported at 6.54, 5.28, 5.02, and 4.01 ppm.[39] The lower chemical shift values of the bipyridyl resonances observed in the $^1$H NMR spectrum of **3** are consistent with a significant reduction in the aromatic character of the bipyridyl ring system and a greater degree of localized alkene-like character to the bond between the carbon atoms to which the protons are bonded. No paramagnetic resonances were observed in the $^1$H NMR spectrum of a $d_8$-THF solution of **2**. They are presumably broadened and lost in the baseline of the spectrum.

To verify the link between aromaticity and the changes in $^1$H NMR chemical shifts, we have computed these parameters using DFT, along with the Nucleus Independent Chemical Shifts (NICS) 1 Å above the center of the bipyridine rings. The calculations reproduce the significant shielding of the aromatic 4,4′-bipy resonances: $\delta_{calc}$ = 8.51 and 7.40 ppm in $\mathbf{1}_{\mathbf{DFT}}$ and 6.20 and 4.66 ppm in $\mathbf{3}_{\mathbf{DFT}}$. A full list of computed and measured chemical shifts is given in the Supporting Information, Table S1. The NICS methodology has emerged as a sensitive probe of aromaticity because the electronic environment of the NICS probe ghost atom (see Experimental Section for details) is highly sensitive to the ring currents characteristic of aromatic systems. For $\mathbf{1}_{\mathbf{DFT}}$, the strongly negative values calculated for the pyridyl rings, −9.78 ppm, are indicative of substantial aromatic character, and are in fact identical to the values computed for the free ligand at the same level of theory (NICS(1) = −9.82 ppm). The aromaticity as measured by NICS is diminished by the addition of one ($\mathbf{2}_{\mathbf{DFT}}$, NICS(1) = −1.88 ppm) and two ($\mathbf{3}_{\mathbf{DFT}}$, NICS(1) = +4.08 ppm) electrons to the $\pi$-system of the ligand. The value for **3** is in fact close to that for the free dianionic bipyridine (+4.94 ppm), and clearly reflects the antiaromatic character of the rings of the dianion.

The topology of the electron density in $\mathbf{1}_{\mathbf{DFT}}$, $\mathbf{2}_{\mathbf{DFT}}$, and $\mathbf{3}_{\mathbf{DFT}}$, analyzed using the atoms in molecules (AIM) methodology, provides an alternative perspective on the changes in the bonding of the rings. Full details of the analysis are presented in Supporting Information, Table S2. The ellipticity at the central C−C bond critical points is a sensitive measure of $\pi$-character: values close to zero indicate a cylindrical symmetric (i.e., $\sigma$) bond, while deviations away from zero indicate increasing $\pi$-character (values in the range 0.18−0.22 are found for aromatic C−C double bonds with partial $\pi$-character). The $\varepsilon$ value for the bridging bond increases dramatically from 0.04 in $\mathbf{1}_{\mathbf{DFT}}$ to 0.34 in $\mathbf{3}_{\mathbf{DFT}}$, again strongly supporting the formulation of the central C−C bridge as double bond. Similarly, the ellipticity of bond 2 within the pyridyl rings increases from 0.22 to 0.37 upon two-electron reduction.

All attempts to measure the standard potentials for the reduction of the neutral complex **1** to the radical anion, $[Zn_2(4,4'\text{-bipy})(mes)_4]^{\bullet-}$, and dianion, $[Zn_2(4,4'\text{-bipy})(mes)_4]^{2-}$, were severely hindered by the extreme air- and moisture-sensitivity of all three species. Such data would have strongly complemented our experimental observations and provide an interesting comparison with respect to the electrochemical data available for 4,4′-bipyridine.[3,4] Despite numerous attempts at recording cyclic voltammetry measurements for **1** we were unable to observe any meaningful signals because of sample decomposition. Despite extensive purging of predried solvents with dinitrogen and the transfer of solutions under an inert atmosphere, we invariably found that samples decomposed prior to the application of an electrical potential. The 0.1 mM solutions required for such measurements are presumably too dilute to allow for the manipulation of the samples on the bench, even under an inert atmosphere.

## CONCLUSIONS

We have isolated and characterized a homologous series of isostructural bipyridyl-bridged dimers, $[Zn_2(4,4'\text{-bipyridine})(mes)_4]^{n-}$ ($n$ = 0 (**1**), 1 (**2**), 2 (**3**)), containing neutral, radical anionic and dianionic forms of the 4,4′-bipyridyl ligand, respectively. Species **2** and **3** represent the first crystallographically authenticated examples of complexes containing the chemically reduced forms of the 4,4′-bipyridyl ligand. The rich redox chemistry of this common ligand may be exploited in coordination polymers and metal organic frameworks giving rise to "switchable" materials where the redox chemistry of ligands and metals are finely matched to facilitate electron transfer between them.

## ASSOCIATED CONTENT

**Supporting Information.** X-ray crystallographic files in CIF format for **1**−**4**. Full experimental and computational details as well as NMR, IR and Raman spectra, powder X-ray diffraction data. This material is available free of charge via the Internet at http://pubs.acs.org.

## AUTHOR INFORMATION

**Corresponding Author**
*E-mail: jose.goicoechea@chem.ox.ac.uk.

## ACKNOWLEDGMENT

We thank the EPSRC and the University of Oxford (studentships to M.I. and T.K.) for financial support of this research. We also thank Dr. Tim Claridge for assistance with NMR spectroscopy, Dr. Jeffrey Harmer for help with EPR spectroscopy, Ragnar Björnsson for helpful comments on NMR calculations, Stephen Boyer (London Metropolitan University) for the elemental analyses, and the University of Oxford for access to OSC, CAESR, and Chemical Crystallography facilities.

## REFERENCES

(1) Carrington, A.; dos Santos-Veiga, J. *Mol. Phys.* **1962**, *5*, 21.
(2) (a) Schmulbach, C. D.; Hinckley, C. C.; Wasmund, D. *J. Am. Chem. Soc.* **1968**, *90*, 6600. (b) Kalyanaraman, V.; Rao, C. N. R.; George, M. V. *J. Chem. Soc. B* **1971**, 2406.
(3) Braterman, P. S.; Song, J.-I. *J. Org. Chem.* **1991**, *56*, 4678.
(4) (a) Roullier, L.; Laviron, E. *Electrochim. Acta* **1978**, *23*, 773. (b) Brown, O. R.; Butterfield, R. J. *Electrochim. Acta* **1982**, *27*, 321.
(5) (a) Ould-Moussa, L.; Poizat, O.; Castellà-Ventura, M.; Buntinx, G.; Kassab, E. *J. Phys. Chem.* **1996**, *100*, 2072. (b) Castellà-Ventura, M.; Kassab, E. *J. Raman Spectrosc.* **1998**, *29*, 511. (c) Kihara, H.; Gondo, Y. *J. Raman Spectrosc.* **1986**, *17*, 263. (d) Lapouge, C.; Buntinx, G.; Poizat, O. *J. Phys. Chem. A* **2002**, *106*, 4168.
(6) (a) Dinolfo, P. H.; Williams, M. E.; Stern, C. L.; Hupp, J. T. *J. Am. Chem. Soc.* **2004**, *126*, 12989. (b) Dinolfo, P. H.; Hupp, J. T. *J. Am. Chem. Soc.* **2004**, *126*, 16814. (c) Bhattacharya, D.; Sathiyendiran, M.; Luo, T.-T.; Chang, C.-H.; Cheng, Y.-H.; Lin, C.-Y.; Lee, G.-H.; Peng, S.-M.; Lu, K.-L. *Inorg. Chem.* **2009**, *48*, 3731.
(7) Denning, M. S.; Irwin, M.; Goicoechea, J. M. *Inorg. Chem.* **2008**, *47*, 6118.
(8) (a) Chirik, P. J.; Wieghardt, K. *Science* **2010**, *327*, 794. (b) Kaim, W. *Coord. Chem. Rev.* **1987**, *76*, 187 and references reported therein.

(c) Hendrickson, D. N.; Pierpont, C. G. In *Spin Crossover in Transition Metal Compounds II*; Springer: Berlin, London, 2004; Vol. 234, p 63. (d) Pierpont, C. G.; Lange, C. W. *Prog. Inorg. Chem.* **1994**, *41*, 331.

(9) (a) Evangelio, E.; Ruiz-Molina, D. *Eur. J. Inorg. Chem.* **2005**, 2957. (b) Rijnberg, E.; Richter, B.; Thiele, K. H.; Boersma, J.; Veldman, N.; Spek, A. L.; van Koten, G. *Inorg. Chem.* **1998**, *37*, 56. (c) Khusniyarov, M. M.; Harms, K.; Burghaus, O.; Sundermeyer, J. *Eur. J. Inorg. Chem.* **2006**, 2985. (d) Gardiner, M. G.; Hanson, G. R.; Henderson, M. J.; Lee, F. C.; Raston, C. L. *Inorg. Chem.* **1994**, *33*, 2456. (e) Lange, C. W.; Conklin, B. J.; Pierpont, C. G. *Inorg. Chem.* **1994**, *33*, 1276. (f) Attia, A. S.; Pierpont, C. G. *Inorg. Chem.* **1997**, *36*, 6184. (g) Sato, O.; Cui, A.; Matsuda, R.; Tao, J.; Hayami, S. *Acc. Chem. Res.* **2007**, *40*, 361. (h) Ohtsu, H.; Tanaka, K. *Angew. Chem., Int. Ed.* **2004**, *43*, 6301.

(10) Chaudhuri, P.; Wieghardt, K. *Prog. Inorg. Chem.* **2001**, *50*, 151.

(11) (a) Wang, K.; Stiefel, E. I. *Science* **2001**, *291*, 106. (b) Harrison, D. J.; Nguyen, N.; Lough, A. J.; Fekl, U. *J. Am. Chem. Soc.* **2006**, *128*, 11026. (c) Kapre, R.; Bothe, E.; Weyhermüller, T.; George, S. D.; Wieghardt, K. *Inorg. Chem.* **2007**, *46*, 5642. (d) Kapre, R.; Ray, K.; Sylvestre, I.; Weyhermüller, T.; George, S. D.; Neese, F.; Wieghardt, K. *Inorg. Chem.* **2006**, *45*, 3499. (e) Ray, K.; George, S. D.; Solomon, E. I.; Wieghardt, K.; Neese, F. *Chem.—Eur. J.* **2007**, *13*, 2783. (f) Ray, K.; Begum, A.; Weyhermüller, T.; Piligkos, S.; Van Slageren, J.; Neese, F.; Wieghardt, K. *J. Am. Chem. Soc.* **2005**, *127*, 4403. (g) Ray, K.; Bill, E.; Weyhermüller, T.; Wieghardt, K. *J. Am. Chem. Soc.* **2005**, *127*, 5641. (h) Ray, K.; Weyhermüller, T.; Neese, F.; Wieghardt, K. *Inorg. Chem.* **2005**, *44*, 5345. (i) Patra, A. K.; Bill, E.; Weyhermüller, T.; Stobie, K.; Bell, Z.; Ward, M. D.; McCleverty, J. A.; Wieghardt, K. *Inorg. Chem.* **2006**, *45*, 6541. (j) Petrenko, T.; Ray, K.; Wieghardt, K.; Neese, F. *J. Am. Chem. Soc.* **2006**, *128*, 4422. (k) Szilagyi, R. K.; Lim, B. S.; Glaser, T.; Holm, R. H.; Hedman, B.; Hodgson, K. O.; Solomon, E. I. *J. Am. Chem. Soc.* **2003**, *125*, 9158. (l) Ray, K.; Weyhermüller, T.; Goossens, A.; Crajé, M. W. J.; Wieghardt, K. *Inorg. Chem.* **2003**, *42*, 4082.

(12) (a) De Bruin, B.; Bill, E.; Bothe, E.; Weyhermüller, T.; Wieghardt, K. *Inorg. Chem.* **2000**, *39*, 2936. (b) Dutta, S. K.; Beckmann, U.; Bill, E.; Weyhermüller, T.; Wieghardt, K. *Inorg. Chem.* **2000**, *39*, 3355. (c) Muresan, N.; Chłopek, K.; Weyhermüller, T.; Neese, F.; Wieghardt, K. *Inorg. Chem.* **2007**, *46*, 5327. (d) Muresan, N.; Weyhermüller, T.; Wieghardt, K. *Dalton Trans.* **2007**, 4390. (e) Chłopek, K.; Bill, E.; Ueller, T. W.; Wieghardt, K. *Inorg. Chem.* **2005**, *44*, 7087. (f) Blanchard, S.; Neese, F.; Bothe, E.; Bill, E.; Weyhermüller, T.; Wieghardt, K. *Inorg. Chem.* **2005**, *44*, 3636.

(13) (a) Lu, C. C.; Bill, E.; Weyhermüller, T.; Bothe, E.; Wieghardt, K. *J. Am. Chem. Soc.* **2008**, *130*, 3181. (b) Wile, B. M.; Trovitch, R. J.; Bart, S. C.; Tondreau, A. M.; Lobkovsky, E.; Milsmann, C.; Bill, E.; Wieghardt, K.; Chirik, P. J. *Inorg. Chem.* **2009**, *48*, 4190.

(14) Lu, C. C.; Bill, E.; Weyhermüller, T.; Bothe, E.; Wieghardt, K. *Inorg. Chem.* **2007**, *46*, 5347.

(15) Cowley, R. E.; Bill, E.; Neese, F.; Brennessel, W. W.; Holland, P. L. *Inorg. Chem.* **2009**, *48*, 4828.

(16) (a) Büttner, T.; Geier, J.; Frison, G.; Harmer, J.; Calle, C.; Schweiger, A.; Schönberg, H.; Grützmacher, H. *Science* **2005**, *307*, 235. (b) Miyazato, Y.; Wada, T.; Muckerman, J. T.; Fujita, E.; Tanaka, K. *Angew. Chem., Int. Ed.* **2007**, *46*, 5728. (c) Mankad, N. P.; Antholine, W. E.; Szilagyi, R. K.; Peters, J. C. *J. Am. Chem. Soc.* **2009**, *131*, 3878.

(17) (a) Blackmore, K. J.; Lal, N.; Ziller, J. W.; Heyduk, A. F. *J. Am. Chem. Soc.* **2008**, *130*, 2728. (b) Haneline, M. R.; Heyduk, A. F. *J. Am. Chem. Soc.* **2006**, *128*, 8410. (c) Chun, H.; Verani, C. N.; Chaudhuri, P.; Bothe, E.; Bill, E.; Weyhermüller, T.; Wieghardt, K. *Inorg. Chem.* **2001**, *40*, 4157. (d) Chaudhuri, P.; Verani, C. N.; Bill, E.; Bothe, E.; Weyhermüller, T.; Wieghardt, K. *J. Am. Chem. Soc.* **2001**, *123*, 2213. (e) Verani, C. N.; Gallert, S.; Bill, E.; Weyhermüller, T.; Wieghardt, K.; Chaudhuri, P. *Chem. Commun.* **1999**, 1747. (f) Chun, M.; Weyhermüller, T.; Bill, E.; Wieghardt, K. *Angew. Chem., Int. Ed.* **2001**, *40*, 2489. (g) Kokatam, S.; Weyhermüller, T.; Bothe, E.; Chaudhuri, P.; Wieghardt, K. *Inorg. Chem.* **2005**, *44*, 3709. (h) Bachler, V.; Olbrich, G.; Neese, F.; Wieghardt, K. *Inorg. Chem.* **2002**, *41*, 4295. (i) Ghosh, P.; Begum, A.; Bill, E.; Weyhermüller, T.; Wieghardt, K. *Inorg. Chem.* **2003**, *42*, 3208. (j) Ghosh, P.; Begum, A.; Herebian, D.; Bothe, E.; Hildenbrand, K.; Weyhermüller, T.; Wieghardt, K. *Angew. Chem., Int. Ed.* **2003**, *42*, 563. (k) Ghosh, P.; Bill, E.; Weyhermüller, T.; Wieghardt, K. *J. Am. Chem. Soc.* **2003**, *125*, 3967. (l) Min, K. S.; Weyhermüller, T.; Wieghardt, K. *Dalton Trans.* **2003**, 1126.

(18) (a) Seidel, W.; Bureger, I. *Z. Anorg. Allg. Chem.* **1981**, *473*, 166. (b) Gridnev, I. D.; Serafimov, J. M.; Quiney, H.; Brown, J. M. *Org. Biomol. Chem.* **2003**, *1*, 3811.

(19) Cosier, J.; Glazer, A. M. *J. Appl. Crystallogr.* **1986**, *19*, 105.

(20) Otwinowski, Z.; Minor, W. . In *Methods in Enzymology*; Academic Press: New York, 1997.

(21) (a) Sheldrick, G. M. *Acta Crystallogr.* **2008**, *A64*, 112. (b) Sheldrick, G. M. *SHELX97, Programs for Crystal Structure Analysis*, release 97-2; Institut für Anorganische Chemie der Universität: Göttingen, Germany, 1998.

(22) Gibbs, S. J.; Johnson, C. S. *J. Magn. Reson.* **1991**, *93*, 395.

(23) Frisch, M. J.; Trucks, G. W.; Schlegel, H. B.; Scuseria, G. E.; Robb, M. A.; Cheeseman, J. R.; Scalmani, G.; Barone, V.; Mennucci, B.; Petersson, G. A.; Nakatsuji, H.; Caricato, M.; Li, X.; Hratchian, H. P.; Izmaylov, A. F.; Bloino, J.; Zheng, G.; Sonnenberg, J. L.; Hada, M.; Ehara, M.; Toyota, K.; Fukuda, R.; Hasegawa, J.; Ishida, M.; Nakajima, T.; Honda, Y.; Kitao, O.; Nakai, H.; Vreven, T.; Montgomery, Jr., J. A.; Peralta, J. E.; Ogliaro, F.; Bearpark, M.; Heyd, J. J.; Brothers, E.; Kudin, K. N.; Staroverov, V. N.; Kobayashi, R.; Normand, J.; Raghavachari, K.; Rendell, A.; Burant, J. C.; Iyengar, S. S.; Tomasi, J.; Cossi, M.; Rega, N.; Millam, J. M.; Klene, M.; Knox, J. E.; Cross, J. B.; Bakken, V.; Adamo, C.; Jaramillo, J.; Gomperts, R.; Stratmann, R. E.; Yazyev, O.; Austin, A. J.; Cammi, R.; Pomelli, C.; Ochterski, J. W.; Martin, R. L.; Morokuma, K.; Zakrzewski, V. G.; Voth, G. A.; Salvador, P.; Dannenberg, J. J.; Dapprich, S.; Daniels, A. D.; Farkas, Ö.; Foresman, J. B.; Ortiz, J. V.; Cioslowski, J.; Fox, D. J. *Gaussian 09*, Revision A.02; Gaussian, Inc.: Wallingford, CT, 2009.

(24) Zhao, Y.; Schultz, N. E.; Truhlar, D. G. *J. Chem. Theory Comput.* **2006**, *2*, 364.

(25) (a) Schäfer, A.; Huber, C.; Ahlrichs, R. *J. Chem. Phys.* **1994**, *100*, 5829. (b) Schäfer, A.; Horn, H.; Ahlrichs, R. *J. Chem. Phys.* **1992**, *97*, 2571.

(26) Bader, R. F. W. *Atoms in Molecules: A Quantum Theory*; Clarendon Press: Oxford, 1990.

(27) Biegler-König, F.; Schönbohm, J. *AIM2000*, version 2.0; Büro für Innovative Software: Bielefeld, Germany, 2002.

(28) (a) Ditchfield, R. *Mol. Phys.* **1974**, *27*, 789. (b) Wolinski, K.; Hinton, J. F.; Pulay, P. J. *J. Am. Chem. Soc.* **1990**, *112*, 8251.

(29) (a) Becke, A. D. *J. Chem. Phys.* **1993**, *98*, 5648. (b) Lee, C.; Yang, W.; Parr, R. G. *Phys. Rev. B* **1988**, *37*, 785. (c) Vosko, S. H.; Wilk, L.; Nusair, M. *Can. J. Phys.* **1980**, *58*, 1200. (d) Stephens, P. J.; Devlin, F. J.; Chabalowski, C. F.; Frisch, M. J. *J. Phys. Chem.* **1994**, *98*, 11623.

(30) Jensen, F. *J. Chem. Theory Comput.* **2008**, *4*, 719.

(31) (a) Jiao, H.; Schleyer, P. V. *J. Phys. Org. Chem.* **1998**, *11*, 655. (b) Schleyer, P. V.; Maerker, C.; Dransfeld, A.; Jiao, H.; Hommes, N. *J. Am. Chem. Soc.* **1996**, *118*, 6317.

(32) See the following reviews and references therein: (a) Yaghi, O. M.; Li, H.; Davis, C.; Richardson, D.; Groy, T. L. *Acc. Chem. Res.* **1998**, *31*, 474. (b) Kitagawa, S.; Kitaura, R.; Noro, S. *Angew. Chem., Int. Ed.* **2004**, *43*, 2334. (c) Biradha, K.; Sarkar, M.; Rajput, L. *Chem. Commun.* **2006**, *40*, 4169.

(33) (a) Soldatov, D. C.; Tinnemans, P.; Enright, G. D.; Ratcliffe, C. I.; Diamente, P. R.; Ripmeester, J. A. *Chem. Mater.* **2003**, *15*, 3826. (b) Liu, S.-H.; Chen, X.-F.; Zhu, X.-H.; Duan, C.-Y.; You, X.-Z. *J. Coord. Chem.* **2001**, *53*, 223. (c) Lai, C. S.; Liu, S.; Tiekink, E. R. T. *CrystEngComm* **2004**, *6*, 221. (d) Chen, X.-F.; Liu, S.-H.; Zhu, X.-H.; Vittal, J. J.; Tan, G.-K.; You, X.-Z. *Acta Crystallogr., Sect. C: Cryst. Struct. Commun.* **2000**, *56*, 42. (e) Diskin-Posner, Y.; Patra, G. K.; Goldberg, I. *Chem. Commun.* **2002**, 1420. (f) Pascu, S. I.; Waghorn, P. A.; Conry, T. D.; Lin, B.; Betts, H. M.; Dilworth, J. R.; Sim, R. B.; Churchill, G. C.; Aigbirhio, F. I.; Warren, J. E. *Dalton Trans.* **2008**, 2107. (g) Konarev, D. V.; Khasanov, S. S.; Slovokhotov, Y. L.; Saito, G.; Lyubovskaya, R. N. *CrystEngComm* **2008**, *10*, 48. (h) Shukla, A. D.; Dave, P. C.; Suresh, E.;

Das, A.; Dastidar, P. *Dalton Trans.* **2000**, 4459. (i) Kleij, A. W.; Kuil, M.; Tooke, D. M.; Lutz, M.; Spek, A. L.; Reek, J. N. H. *Chem.—Eur. J.* **2005**, *11*, 4743. (j) Litvinov, A. L.; Konarev, D. V.; Kovalevsky, A. Y.; Neretin, I. S.; Coppens, P.; Lyubovskaya, R. N. *Cryst. Growth Des.* **2005**, 1807. (k) Manohar, A.; Ramalingam, K.; Bocelli, G.; Righi, L. *Inorg. Chim. Acta* **2001**, *314*, 177. (l) Benson, R. E.; Ellis, C. A.; Lewis, C. E.; Tiekink, E. R. T. *CrystEngComm* **2007**, *9*, 930. (m) Tao, J.; Yin, X.; Zheng, L. S.; Ng, S. W. *Main Group Met. Chem.* **2002**, *25*, 321. (n) Croitor, L.; Coropceanu, E. B.; Jeanneau, E.; Dementiev, I. V.; Goglidze, T. I.; Chumakov, Y. M.; Fonarim, M. S. *Cryst. Growth Des.* **2009**, *9*, 5233.

(34) (a) Hasenzahl, S.; Kaim, W.; Stahl, T. *Inorg. Chim. Acta* **1994**, *225*, 23. (b) Shenai-Khatkhate, D. V.; Orrell, E. D.; Mullin, J. B.; Cupertino, D. C.; Cole-Hamilton, D. J. *J. Cryst. Growth* **1986**, *77*, 27.

(35) (a) Kaim, W. *Inorg. Chim. Acta* **1981**, *53*, L151. (b) Kaim, W. *J. Organomet. Chem.* **1984**, *262*, 171. (c) Gross, R.; Kaim, W. *Angew. Chem., Int. Ed* **1985**, *24*, 856.

(36) Krieger, M.; Geiseler, G.; Harms, K.; Merle, J.; Massa, W.; Dehnicke, K. *Z. Anorg. Allg. Chem.* **1998**, *624*, 1387.

(37) Irwin, M.; Jenkins, R. K.; Denning, M. S.; Krämer, T.; Grandjean, F.; Long, G. J.; Herchel, R.; McGrady, J. E.; Goicoechea, J. M. *Inorg. Chem.* **2010**, *49*, 6160.

(38) Gore-Randall, E.; Irwin, M.; Denning, M. S.; Goicoechea, J. M. *Inorg. Chem.* **2009**, *48*, 8304.

(39) Fedushkin, I. L.; Petrovskaya, T. V.; Girgsdies, F.; Köhn, R. D.; Bochkarev, M. N.; Schumann, H. *Angew. Chem., Int. Ed.* **1999**, *38*, 2262.